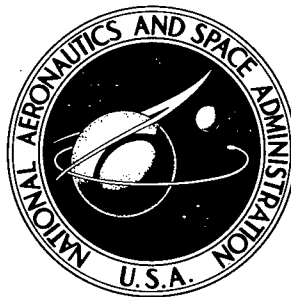


3057139 P

NASA TECHNICAL NOTE



NASA TN D-2461

NASA TN D-2461

PROPERTY OF:
AMPTIAC LIBRARY

57139

AMPTIAC LIBRARY

DISTRIBUTION STATEMENT A
Approved for Public Release
Distribution Unlimited

PROPERTY OF:

ANALYSIS OF BONDING MECHANISM BETWEEN PLASMA-SPRAYED TUNGSTEN AND A STAINLESS STEEL SUBSTRATE

by William A. Spitzig and Salvatore J. Grisaffe

Lewis Research Center

Cleveland, Ohio

20011221 184

ANALYSIS OF BONDING MECHANISM BETWEEN PLASMA-SPRAYED
TUNGSTEN AND A STAINLESS STEEL SUBSTRATE

By William A. Spitzig and Salvatore J. Grisaffe

Lewis Research Center
Cleveland, Ohio

**Reproduced From
Best Available Copy**

NATIONAL AERONAUTICS AND SPACE ADMINISTRATION

For sale by the Office of Technical Services, Department of Commerce,
Washington, D.C. 20230 -- Price \$0.50

ANALYSIS OF BONDING MECHANISM BETWEEN PLASMA-SPRAYED

TUNGSTEN AND A STAINLESS STEEL SUBSTRATE

by William A. Spitzig and Salvatore J. Grisaffe

Lewis Research Center

T. FRA

SUMMARY

Experimental results show that alloy bonds can be formed between tungsten particles and a 304 stainless steel substrate during the plasma-spraying process. [A heat-transfer analysis has demonstrated the feasibility of raising the temperature of a 304 stainless steel substrate directly beneath a tungsten particle to temperatures near the melting range of the substrate and thereby giving rise to high diffusion rates, which promote bonding.] This local temperature rise occurs when the tungsten particle gives up its energy, obtained as a result of traveling in the plasma stream, to a small region in the stainless steel directly beneath the particle. This region is raised to temperatures near its melting range and cooled to around 500° F in approximately 10⁻⁵ second.

INTRODUCTION

W, 55

The bond strength of a plasma-sprayed coating is generally attributed to mechanical interlocking of the deposited particles with a substrate having a roughened surface. In previous work by the authors (ref. 1), however, the nature of the coating-substrate bond was studied in the absence of mechanical interlocking; that is, the substrate surfaces were metallographically polished. In that study plasma-sprayed tungsten particles exhibited excellent adherence when sprayed onto a 304 stainless steel substrate. This result was rather surprising, since the surface of the substrate was metallographically polished and the substrate was not heated prior to spraying. This seems to indicate that the temperature in the stainless steel underneath the tungsten particle can become high enough to allow bonding to occur between the particle and the substrate, even though the overall temperature of the substrate is near room temperature. The purpose of this investigation was to analyze the bonding mechanism between plasma-sprayed tungsten and 304 stainless steel.

This report gives the experimentally observed metallurgical nature of the tungsten - 304 stainless steel interface and an analysis of the temperature distribution in the stainless steel substrate as a function of both time and distance beneath the interface. The analysis is essentially an energy balance in which the energy of a tungsten particle (thermal and kinetic) is assumed to

be transferred to the stainless steel substrate. The temperature distribution in the substrate is then obtained by a standard solution to the classical differential equation for heat conduction. The appearance of the tungsten - stainless steel interface is discussed in the light of the analytical results.

MATERIALS AND PROCEDURES

The particle size of the tungsten powder ranged from 62 to 30 microns. The substrate material was 304 stainless steel. Spraying was performed in air with a plasma spray torch operating at the following fixed conditions:

Spray nozzle inside diameter, in.	7/32
Current, amp	450
Voltage, v	60
Plasma-nitrogen flow rate, cu ft/hr ¹	80
Plasma-hydrogen flow rate, cu ft/hr ¹	10
Carrier-nitrogen flow rate, cu ft/hr ¹	10
Auger-type powder hopper setting	11.9

The 304 stainless steel was cut into 1- by 1-inch squares approximately 1/8 inch thick. These squares were mounted in self-curing exothermic plastic and metallographically polished to produce a scratch-free surface. These squares were left in the original polishing mounts, and the tungsten particles were deposited on them by moving the mounts at right angles through the plasma

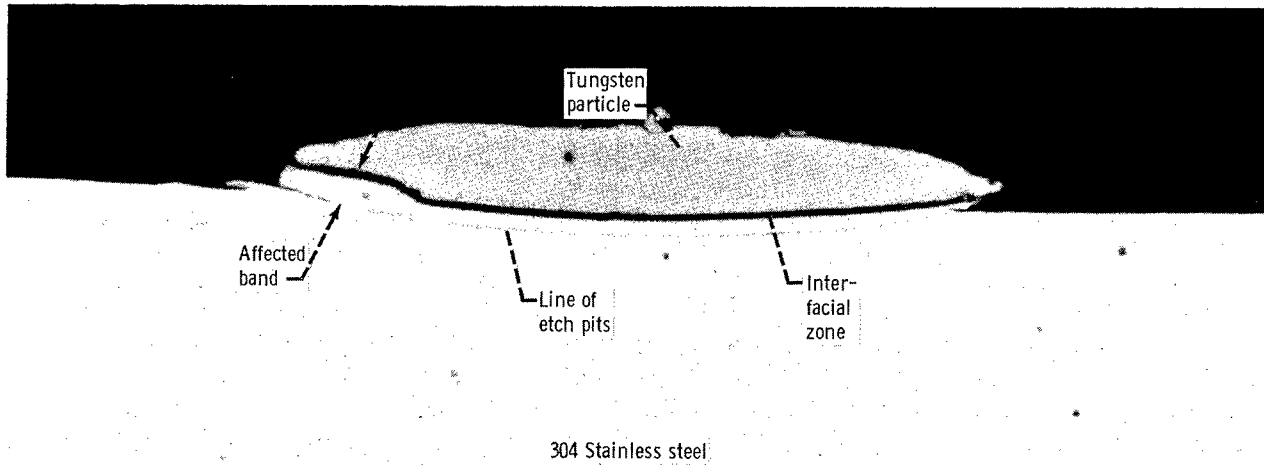


Figure 1. - Cross-sectional view of tungsten particle on 304 stainless steel substrate for 3-inch torch-to-substrate distance. Etchant, oxalic acid. X1000.

¹Standard cubic feet per hour.

stream at a rate of approximately 1 foot per second. At this rate, particles were deposited on the substrate in such a manner that individual particles could be examined. This method also prevented the substrate from being heated to any great extent from the plasma during the deposition process.

RESULTS AND DISCUSSION

Experimental Observations

A typical cross section of a tungsten particle on the stainless steel substrate is shown in figure 1. This figure is for a specimen sprayed at a 3-inch torch-to-substrate distance. Specimens sprayed at other torch-to-substrate distances (4 to 6 in.) also exhibited excellent adherence between the tungsten particles and the stainless steel substrates.

Close examination of figure 1 shows that directly under the particle an interfacial zone exists, and beneath this zone a line of discontinuity is present that follows the contour of the interfacial zone. Examination of this zone in the unetched condition showed that no voids or oxide films were observable between the particle and the substrate. The curved interface between the tungsten particle and the stainless steel substrate is in direct contrast to the relatively straight line type of interface that is usually present between a tungsten particle and a tungsten substrate (ref. 2).

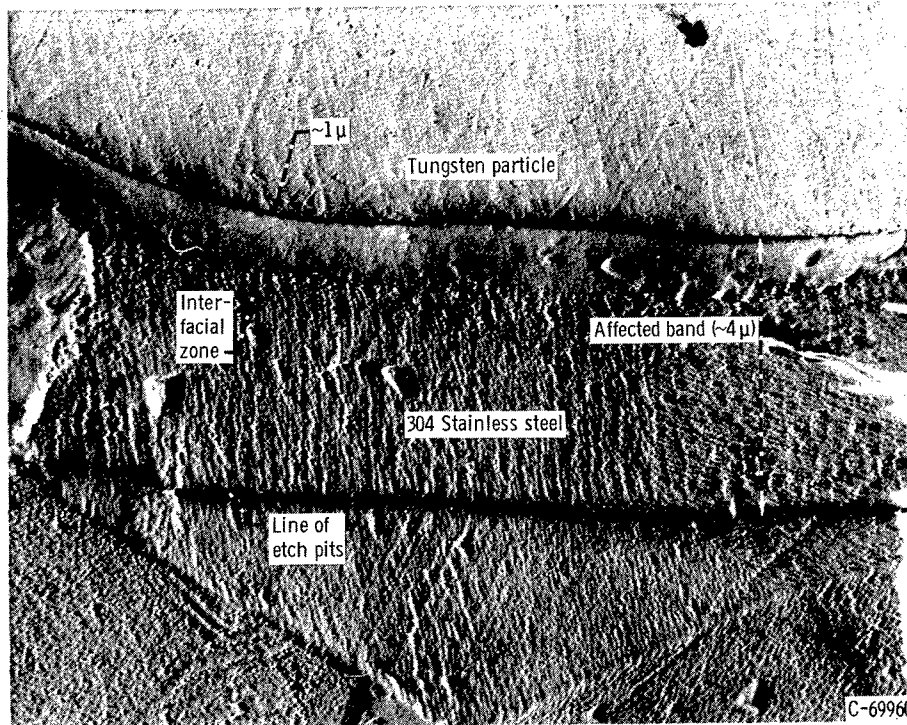


Figure 2. - Electron micrograph of cross section of coating and substrate for 3-inch torch-to-substrate distance. Etchant, oxalic acid. X9600.

Figure 2 is an electron micrograph ($\times 9600$) of the region beneath the tungsten particle showing the interfacial zone and line of discontinuity in the substrate. Directly beneath the tungsten particle is an interfacial zone approximately 1 micron in depth. Approximately 4 microns below the tungsten particle is the line of discontinuity. The stainless steel between this line and the tungsten particle is designated the affected band. This line of discontinuity was found, by higher magnification electron micrographs, to be a row of etch pits. The cause of these etch pits is not apparent at present.

From figures 1 and 2 it is apparent that a reaction has occurred between the tungsten and the stainless steel that resulted in the interfacial zone directly beneath the particle.

Electron probe traverses across the tungsten stainless steel interface showed that concentration gradients of iron, chromium, nickel, and tungsten exist across the whole affected band. Because of the smallness of this affected band (approximately 4μ), no significant quantitative measurements of the gradient through the region could be obtained. An average of readings in the center of the affected band, however, showed a tungsten concentration of about 6 weight percent.

Microhardness measurements with a 5-gram load across the interface showed that the affected band (diamond pyramid hardness, 305) was intermediate in hardness between the tungsten particle (DPH, 400) and the stainless steel substrate (DPH, 205). This increase in hardness over that of the stainless steel substrate could have resulted from solid solution hardening or the presence of unresolvable intermetallic compounds.

Metallographic, microprobe, and hardness measurements indicate that the bond between a tungsten particle and the stainless steel substrate is of the alloy type as a result of the diffusion that occurs after the hot tungsten particle impinges on the stainless steel and before it cools down to room temperature. Therefore, even though the hot particles are rapidly cooled on impact, the low thermal conductivity of the stainless steel apparently allows diffusion to occur over distances in the range of 2 to 3 microns. Such a diffusion bond obtained in the short time involved is surprising. For this reason an energy balance analysis was made in an effort to determine the temperature in the stainless steel substrate directly beneath the particle. This was done to determine if it is possible for the stainless steel substrate to attain localized temperatures that are sufficiently high to enhance diffusion rates and therefore allow diffusion to occur over distances of 2 to 3 microns.

Heat-Transfer Analysis

As the tungsten particles are traveling in the plasma stream, they are heated to a high temperature. The heat that must be absorbed Q by n moles of material with a specific heat c_p to increase the temperature of the material from T_1 to T_2 is

$$Q = n \int_{T_1}^{T_2} c_p dT \quad (1)$$

where c_p is a function of temperature. This equation assumes that no transformations occur on heating between T_1 and T_2 , and for tungsten this assumption is valid up to its melting point (6170° F).

A previous investigation (ref. 1) showed that the average temperature of the tungsten particles (particle size range, 62 to 30 μ) traveling in the plasma stream was approximately 3550° F when they reached a point 3 inches from the nozzle. It was also determined (ref. 1) that at this distance the temperature of the center of the tungsten particle should be the same as that of the surface for particle sizes less than 100 microns. (The particle size of the tungsten powder used in the investigation reported herein was 62 to 30 μ .)

The tungsten particle shown in figure 1, which is typical of all the particles observed, can be approximated by a disk with a diameter of 0.094 millimeter and a height of 0.008 millimeter. Since the tungsten particles become spherical while passing through the plasma stream (ref. 3), the original size of the disklike tungsten particle in figure 1 was calculated to be a 47-micron sphere.

[The heat absorbed by a 47-micron tungsten particle, while traveling in the plasma stream, as a result of its temperature being increased from room temperature to 3550° F] can be calculated from equation (1). When values of c_p as a function of temperature from reference 4 were used, the heat absorbed [was calculated to be 7.5×10^{-5} calorie.] (See appendix A.)

[The average velocity of the tungsten particles as they impinge on the stainless steel substrate 3 inches from the torch has been determined to be about 240 feet per second.] (ref. 1). [Therefore, the kinetic energy that a 47-micron tungsten particle attains just as it impinges on the substrate is about 0.07×10^{-5} calorie. Thus the total energy of the tungsten particle Q' is 7.57×10^{-5} calorie.]

If the stainless steel substrate is assumed to be a homogeneous isotropic solid with constant thermal properties, the differential equation of heat conduction can be solved to give an equation (ref. 5) that gives the temperature in the stainless steel beneath the particle as a function of distance from the surface and time:

$$\Delta T = \frac{Q'}{2\pi a^2 \rho c_p \sqrt{\pi K t}} \left[1 - \exp\left(-\frac{a^2}{4Kt}\right) \right] \exp\left(-\frac{z^2}{4Kt}\right) \quad (2)$$

where

ΔT increase in temperature above room temperature, °K

Q' total heat units supplied from tungsten particle, cal

- a radius of disk-shaped particle, cm
- ρ density, g/cm³
- c_p specific heat, cal/(g)(°K)
- K thermal diffusivity, k/ $c_p\rho$, cm²/sec
- k thermal conductivity, cal/(sec)(cm)(°K)
- t time, sec
- z distance in substrate perpendicular to surface and directly below center of particle, cm

The use of this equation for the case at hand involves the additional assumption that the tungsten particle acts as an instantaneous disk source of thermal energy. The actual situation is much more complex than this; however, it was felt that this analysis would yield results that would serve as first approximations. The source gives up its energy to the stainless steel substrate directly beneath the particle over a circular area of radius a. Equation (2) gives the temperature distribution in the stainless steel as a result of this energy being supplied at its surface.

In the case of 304 stainless steel the assumption, inherent in the derivation of equation (2), that the thermal diffusivity remains constant is not a great source of error since both the thermal conductivity and the specific heat increase at essentially the same rate with temperature (ref. 6). The effect of thermal expansion in the stainless steel is neglected in this equation, and the density was taken as constant over the whole temperature range. The following table lists the values of the thermal diffusivity over a temperature range where applicable data were found:

Temperature, T, °F	Thermal conductivity, k, cal/(sec)(cm)(°K)	Specific heat, c_p , cal/(g)(°K)	Density, ρ , g/cm ³	Thermal diffusivity, K, cm ² /sec
	(a)	(a)	(b)	
100	32.2×10 ⁻³	0.110	7.9	4.28×10 ⁻²
800	49.6	.137	↓	4.59
1600	62.0	.154		5.10
2400	71.0	.180		5.01

^aData for 301 stainless steel taken from ref. 6 (appropriate data were not available for 304 stainless steel).

^bData from ref. 7.

^cExtrapolated.

From this table it is apparent that the ratio does not vary considerably and the maximum variation is about 19 percent. This variation is not considered significant since the available thermal data are not usually very accurate. Also, since the thermal diffusivity enters into equation (2) as a square root or as an exponential term, the effect of the slight difference in its value is further reduced.

Assuming an ideal case, where all the energy contained in the tungsten particle, thermal and kinetic ($Q' = 7.57 \times 10^{-5}$ cal), is transferred to the stainless steel substrate directly beneath the particle, and using values of $a = 4.7 \times 10^{-3}$ centimeter, $\rho = 7.9$ grams per cubic centimeter, $c_p = 0.180$ calorie per gram $^{\circ}\text{K}$, and $K = 4.75 \times 10^{-2}$ square centimeter per second (an average value from the table) enable calculation of the temperature under the particle as a function of depth and time. Substituting these values in equation (2) and simplifying give the following relation for T:

$$T = \frac{0.99}{\sqrt{t}} \left[1 - \exp\left(-\frac{1.16 \times 10^{-4}}{t}\right) \right] \exp\left(-\frac{5.27 z^2}{t}\right) + 298 \quad (3)$$

where T, z, and t have the units $^{\circ}\text{K}$, centimeters, and seconds, respectively. (See appendix B.)

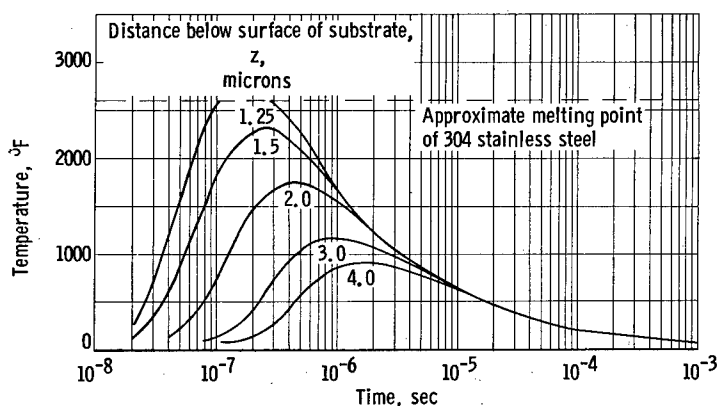


Figure 3. - Calculated temperature distribution in 304 stainless steel substrate beneath tungsten particle as function of time and distance below surface.

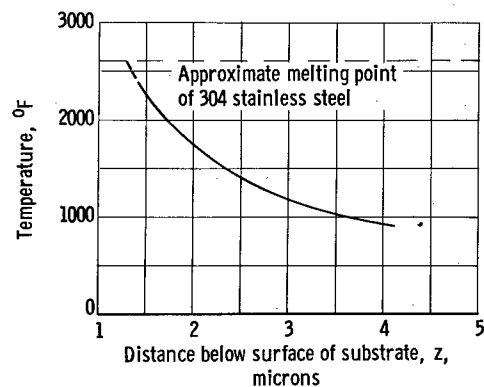


Figure 4. - Calculated maximum temperature in 304 stainless steel substrate beneath tungsten particle as function of depth.

The temperatures at various distances in the stainless steel substrate as a function of time, as calculated from equation (3) are shown in figure 3. (A sample calculation is shown in appendix B.) Figure 4 shows the maximum temperature that the substrate underneath the particle can attain at various distances below the surface. These

calculations indicate that very high localized temperatures can be attained in the stainless steel. From these figures it is apparent that at distances to about 1.3 microns below the surface the stainless steel can be raised to its melting range. This is the maximum depth to which the substrate can be heated to its melting range, since the ideal case was assumed, and in general the depth would be reduced. This distance was calculated on the assumption that the liquid and the solid have the same thermal properties and a negligible heat of fusion. (It should be noted that the time for heating up and cooling down to approximately 500°F is of the order of 10^{-5} second.)

As a rough check on the temperature distribution, a calculation was made to see if sufficient energy was available from the tungsten particle in cooling from 3550° to 2600° F to raise the appropriate volume of stainless steel to its melting point (approx. 2600° F). The stainless steel actually has a melting range of approximately 2550° to 2650° F, but an average value of 2600° F was taken as the melting point for simplicity. The volume of stainless steel used was that of a disk of radius a (4.7×10^{-3} cm) with a height of 1.3 microns. The results of the calculation (appendixes A and C) showed that sufficient energy was available from the tungsten particle in cooling from 3550° to 2600° F to raise this volume of stainless steel to its melting point and cause it to melt. There was actually a 14-percent excess of energy available. That is, the energy given up by the tungsten particle in cooling from 3550° to 2600° F was 2.2×10^{-5} calorie (appendix A), and the energy needed to raise the disk of stainless steel to its melting point and cause it to melt was 1.9×10^{-5} calorie (appendix C). This rough check shows good agreement with the analysis in that the energy given up by the tungsten particle in cooling from 3550° to 2600° F is approximately that needed to melt a disk of stainless steel under the particle having a height of 1.3 microns as calculated from the analysis. The energy required to heat and melt this 1.3-micron disk of stainless steel (1.9×10^{-5} cal) was only about 25 percent of the total energy the tungsten particle had on impact (7.57×10^{-5} cal). Therefore, there was still a considerable amount of energy available for promoting thermal diffusion and consequently heating the substrate to greater depths. An approximate calculation also showed that the amount of heat lost by the particle through radiation was negligible during the short time that the particle was at temperature ($\sim 10^{-5}$ sec.)

→ P 9

Discussion of Experimental and Analytical Results

The results from the heat-transfer analysis showed that the stainless steel directly beneath the tungsten particle can be raised to its melting range to a distance of 1.3 microns below the particle. Microprobe analysis showed that a definite interaction zone existed under the tungsten particle, and the zone was approximately 4 microns in depth. Microstructure analysis indicated that an interfacial zone approximately 1 micron thick existed under the particle. This zone etched in the same way as the tungsten particle which suggested that it contained a high percentage of tungsten and therefore must have been at temperatures near its melting range to allow such high rates of diffusion. High-magnification metallographic examination of the interfacial zone gave no obvious structural evidence to confirm the analytical result that melting can occur in a 1.3-micron layer of the substrate. Therefore a comparison of the experimental and analytical results indicates that one of the following cases is true:

- (1) The calculated temperature is high, and the surface of the substrate reached a temperature near its melting range, as evidenced by the 1-micron interfacial zone, but it did not melt.
- (2) The surface of the substrate reached its melting range as calculated, but the material that was molten was expelled or was not resolvable.

Most of the experimental evidence supports case 1, but some support for case 2 is the curved interface between the particle and the substrate, which gives the impression that some of the stainless steel was displaced. There is not sufficient experimental evidence, however, to decide for certain which of the two cases is correct. In either case the only question is that of whether or not actual melting occurs. Both the experimental and the analytical results are in agreement on the fact that the substrate beneath the particle can be raised to temperatures near its melting range.

[CONCLUSIONS]

From an analysis of the bonding mechanism between plasma-sprayed tungsten and a 304 stainless steel substrate the following conclusions were drawn:

1. Alloy bonds can be formed between tungsten particles and the stainless steel substrate during the plasma spraying process.
2. The bonds are achieved by rapid localized diffusion in the stainless steel directly beneath the tungsten particle.
3. Rapid localized diffusion occurs as a result of heating of the substrate directly beneath the tungsten particle to temperatures near the melting range of the substrate; diffusion occurs during times of the order of 10^{-5} second.
4. The localized temperature rise results when the tungsten particle gives up its energy, obtained as a result of traveling in the plasma stream, to a small region in the stainless steel directly beneath the particle.

end.

Lewis Research Center
National Aeronautics and Space Administration
Cleveland, Ohio, June 25, 1964

APPENDIX A

CALCULATION OF HEAT CONTENT AND TEMPERATURE

The heat content of an impinging tungsten particle is calculated from the equation

$$Q = n \int_{T_1}^{T_2} c_p dT$$

where

n moles of tungsten

T_1 room temperature, 298° K

T_2 temperature of impinging particle, 2223° K (3550° F)

c_p specific heat of tungsten, $5.74 + 0.76 \times 10^{-3} T$ (ref. 5), cal/(mole)(°K)

For a 47-micron sphere, the volume is

$$V = \frac{\pi d^3}{6} = 55 \times 10^{-9} \text{ cm}^3$$

where d is the diameter of the sphere. The mass, from the equation

$$m = \rho V$$

with the density ρ equal to 19.3 grams per cubic centimeter, is

$$m = 1060 \times 10^{-9} \text{ g}$$

The number of moles, from the equation

$$n = \frac{m}{\text{atomic weight}}$$

with the atomic weight equal to 183.9, is

$$n = 5.8 \times 10^{-9} \text{ mole}$$

The heat content of an impinging particle is then

$$Q = 5.8 \times 10^{-9} \int_{298}^{2223} (5.74 + 0.76 \times 10^{-3} T) dT$$
$$= 7.5 \times 10^{-5} \text{ cal}$$

The heat given up by a tungsten particle in cooling from 3550° F (2223° K) to 2600° F (1698° K) is

$$Q = 5.8 \times 10^{-9} \int_{1698}^{2223} (5.74 + 0.76 \times 10^{-3} T) dT$$
$$= 2.2 \times 10^{-5} \text{ cal}$$

APPENDIX B

HEAT TRANSFER ANALYSIS

The equation for calculating the heat-transfer in the stainless steel beneath the impinging particle is

$$\Delta T = \frac{Q'}{2\pi a^2 \rho c_p \sqrt{\pi K t}} \left[1 - \exp\left(-\frac{a^2}{4Kt}\right) \right] \exp\left(-\frac{z^2}{4Kt}\right)$$

where

ΔT increase in temperature above room temperature, $^{\circ}\text{K}$

Q' total heat units supplied from tungsten particle, cal

a radius of disk-shaped particle, cm

ρ density, g/cm^3

c_p specific heat, $\text{cal}/(\text{g})(^{\circ}\text{K})$

K thermal diffusivity, $\text{k}/c_p \rho$, cm^2/sec

k thermal conductivity, $\text{cal}/(\text{sec})(\text{cm})(^{\circ}\text{K})$

t time, sec

z distance in substrate perpendicular to surface and directly below center of particle, cm

In order to calculate the temperature from equation (2), the total heat supplied from the tungsten particle Q' is defined as

$$Q' = Q + W$$

where Q is the heat content of an impinging particle, equal to 7.5×10^{-5} calorie, and W is the kinetic energy of the tungsten particle on impact, equal to 0.07×10^{-5} calorie. Thus,

$$Q' = 7.5 \times 10^{-5} + 0.07 \times 10^{-5} = 7.57 \times 10^{-5} \text{ cal}$$

With the following values substituted in equation (2)

$$a = 4.7 \times 10^{-3} \text{ cm}$$

$$\rho = 7.9 \text{ g}/\text{cm}^3$$

$$c_p = 0.180 \text{ cal}/(\text{g})(^{\circ}\text{K})$$

$K = 4.75 \times 10^{-2} \text{ cm}^2/\text{sec}$ (average value from table on p. 6)

the equation becomes

$$\Delta T = \frac{7.57 \times 10^{-5}}{2\pi(4.7 \times 10^{-3})^2(7.9)(0.180) \sqrt{\pi(4.75 \times 10^{-2})t}} \times \left\{ 1 - \exp\left[-\frac{(4.7 \times 10^{-3})^2}{4(4.75 \times 10^{-2})t}\right] \right\} \exp\left[-\frac{z^2}{4(4.75 \times 10^{-2})t}\right]$$

which reduces to the relation

$$T = \frac{0.99}{\sqrt{t}} \left[1 - \exp\left(-\frac{1.16 \times 10^{-4}}{t}\right) \right] \exp\left(\frac{-5.27 z^2}{t}\right) + 298$$

where T , z , and t are expressed in $^{\circ}\text{K}$, centimeters, and seconds, respectively.

For example, with t equal to 1×10^{-7} second and z equal to 1.5×10^{-4} centimeter,

$$\begin{aligned} T &= \frac{0.99}{\sqrt{1 \times 10^{-7}}} \left[1 - \exp\left(-\frac{1.16 \times 10^{-4}}{1 \times 10^{-7}}\right) \right] \exp\left[-\frac{(5.27)(1.5 \times 10^{-4})^2}{1 \times 10^{-7}}\right] + 298 \\ &= 3125(1 - 0)(0.306) + 298 \\ &= 1253^{\circ} \text{ K (or } 1795^{\circ} \text{ F)} \end{aligned}$$

APPENDIX C

HEAT NEEDED TO RAISE DISK OF 304 STAINLESS STEEL

TO ITS MELTING POINT AND TO CAUSE MELTING

The melting point of 304 stainless steel is taken as 2600° F (1698° K). If the radius of the disk is 4.7×10^{-3} centimeter, the height of the disk is 1.3×10^{-4} centimeter, and the density is 7.9 grams per cubic centimeter, the mass (density \times volume) is

$$m = 714 \times 10^{-10} \text{ g}$$

For an average specific heat c_p of 0.145 calorie per gram °K and a temperature change ΔT of 1400° K (1698° - 298° K), the heat needed to raise a stainless steel disk to its melting point

$$Q_t = mc_p \Delta T$$

is

$$Q_t = 1.45 \times 10^{-5} \text{ cal}$$

The heat needed to melt the disk is

$$Q_M = \Delta H_{Fe} n \frac{(\text{kcal})(\text{moles})}{\text{mole}}$$

where ΔH_{Fe} is the heat of melting for iron. This value was used for the calculation since the heat of melting for 304 stainless steel was not available. It was also assumed that the only transformation that occurred on heating was that of melting. For 304 stainless steel this is a valid assumption.

Since

$$\Delta H_{Fe} = 3700 \text{ cal/mole (ref. 8)}$$

and, with atomic weight equal to 56 g,

$$n = \frac{m}{\text{atomic weight}} = 12.7 \times 10^{-10} \text{ mole}$$

$$Q_M = 0.47 \times 10^{-5} \text{ cal}$$

Then the total heat needed to raise the disk temperature to the melting point and to cause melting is

$$Q_T = Q_t + Q_M = 1.9 \times 10^{-5} \text{ cal}$$

REFERENCES

1. Grisaffe, Salvatore J., and Spitzig, William A.: Preliminary Investigation of Particle-Substrate Bonding of Plasma-Sprayed Materials. NASA TN D-1705, 1963.
2. Grisaffe, S. J., and Spitzig, W. A.: Observations on Metallurgical Bonding Between Plasma Sprayed Tungsten and Hot Tungsten Substrates. ASM Trans. Quarterly, vol. 56, no. 3, Sept. 1963, pp. 618-628.
3. Spitzig, W. A.: Sintering of Arc Plasma Sprayed Tungsten. M.S. Thesis, Case Inst. Tech., 1962.
4. Kelley, K. K.: Contributions to the Data on Theoretical Metallurgy. XIII. High-Temperature Heat-Content, Heat-Capacity, and Entropy Data for the Elements and Inorganic Compounds. Bull. 584, Bur. Mines, 1960.
5. Carslaw, H. S., and Jaeger, J. C.: Conduction of Heat in Solids. Second ed., Univ. Press (Oxford), 1959.
6. Wolfe, G. W., and Arne, V. L.: Thermal Properties of Solids. Rep. E9R-12073, Chance Vought Aircraft, Inc., Sept. 1, 1959.
7. Lyman, Taylor, ed.: Metals Handbook. Vol. 1, Eighth ed., ASM, 1961.
8. Kubaschewski, O., and Evans, E. LL.: Metallurgical Thermochemistry. Third Ed., Pergamon Press, 1958.

NASA TN D-2461

National Aeronautics and Space Administration.
ANALYSIS OF BONDING MECHANISM BETWEEN
PLASMA-SPRAYED TUNGSTEN AND A STAINLESS
STEEL SUBSTRATE. William A. Spitzig and
Salvatore J. Grisaffe. September 1964. 15p. OTS
price, \$0.50. (NASA TECHNICAL NOTE D-2461)

Experimental results show that alloy bonds can be formed between tungsten particles and a 304 stainless steel substrate during the plasma-spraying process. A heat-transfer analysis has demonstrated the feasibility of raising the temperature of the stainless steel substrate directly beneath the tungsten particle to temperatures near the melting range of the substrate and thereby giving rise to high diffusion rates, which promote bonding. This temperature rise occurs because the tungsten particle gives up its energy on impact to a small region in the stainless steel directly beneath the particle.

- I. Spitzig, William A.
- II. Grisaffe, Salvatore J.
- III. NASA TN D-2461

NASA

NASA TN D-2461

National Aeronautics and Space Administration.
ANALYSIS OF BONDING MECHANISM BETWEEN
PLASMA-SPRAYED TUNGSTEN AND A STAINLESS
STEEL SUBSTRATE. William A. Spitzig and
Salvatore J. Grisaffe. September 1964. 15p. OTS
price, \$0.50. (NASA TECHNICAL NOTE D-2461)

Experimental results show that alloy bonds can be formed between tungsten particles and a 304 stainless steel substrate during the plasma-spraying process. A heat-transfer analysis has demonstrated the feasibility of raising the temperature of the stainless steel substrate directly beneath the tungsten particle to temperatures near the melting range of the substrate and thereby giving rise to high diffusion rates, which promote bonding. This temperature rise occurs because the tungsten particle gives up its energy on impact to a small region in the stainless steel directly beneath the particle.

NASA

NASA TN D-2461

National Aeronautics and Space Administration.
ANALYSIS OF BONDING MECHANISM BETWEEN
PLASMA-SPRAYED TUNGSTEN AND A STAINLESS
STEEL SUBSTRATE. William A. Spitzig and
Salvatore J. Grisaffe. September 1964. 15p. OTS
price, \$0.50. (NASA TECHNICAL NOTE D-2461)

Experimental results show that alloy bonds can be formed between tungsten particles and a 304 stainless steel substrate during the plasma-spraying process. A heat-transfer analysis has demonstrated the feasibility of raising the temperature of the stainless steel substrate directly beneath the tungsten particle to temperatures near the melting range of the substrate and thereby giving rise to high diffusion rates, which promote bonding. This temperature rise occurs because the tungsten particle gives up its energy on impact to a small region in the stainless steel directly beneath the particle.

- I. Spitzig, William A.
- II. Grisaffe, Salvatore J.
- III. NASA TN D-2461

NASA

NASA TN D-2461

National Aeronautics and Space Administration.
ANALYSIS OF BONDING MECHANISM BETWEEN
PLASMA-SPRAYED TUNGSTEN AND A STAINLESS
STEEL SUBSTRATE. William A. Spitzig and
Salvatore J. Grisaffe. September 1964. 15p. OTS
price, \$0.50. (NASA TECHNICAL NOTE D-2461)

Experimental results show that alloy bonds can be formed between tungsten particles and a 304 stainless steel substrate during the plasma-spraying process. A heat-transfer analysis has demonstrated the feasibility of raising the temperature of the stainless steel substrate directly beneath the tungsten particle to temperatures near the melting range of the substrate and thereby giving rise to high diffusion rates, which promote bonding. This temperature rise occurs because the tungsten particle gives up its energy on impact to a small region in the stainless steel directly beneath the particle.

NASA

NASA TN D-2461

National Aeronautics and Space Administration.
ANALYSIS OF BONDING MECHANISM BETWEEN
PLASMA-SPRAYED TUNGSTEN AND A STAINLESS
STEEL SUBSTRATE. William A. Spitzig and
Salvatore J. Grisaffe. September 1964. 15p. OTS
price, \$0.50. (NASA TECHNICAL NOTE D-2461)

Experimental results show that alloy bonds can be formed between tungsten particles and a 304 stainless steel substrate during the plasma-spraying process. A heat-transfer analysis has demonstrated the feasibility of raising the temperature of the stainless steel substrate directly beneath the tungsten particle to temperatures near the melting range of the substrate and thereby giving rise to high diffusion rates, which promote bonding. This temperature rise occurs because the tungsten particle gives up its energy on impact to a small region in the stainless steel directly beneath the particle.

- I. Spitzig, William A.
- II. Grisaffe, Salvatore J.
- III. NASA TN D-2461

NASA

NASA TN D-2461

National Aeronautics and Space Administration.
ANALYSIS OF BONDING MECHANISM BETWEEN
PLASMA-SPRAYED TUNGSTEN AND A STAINLESS
STEEL SUBSTRATE. William A. Spitzig and
Salvatore J. Grisaffe. September 1964. 15p. OTS
price, \$0.50. (NASA TECHNICAL NOTE D-2461)

Experimental results show that alloy bonds can be formed between tungsten particles and a 304 stainless steel substrate during the plasma-spraying process. A heat-transfer analysis has demonstrated the feasibility of raising the temperature of the stainless steel substrate directly beneath the tungsten particle to temperatures near the melting range of the substrate and thereby giving rise to high diffusion rates, which promote bonding. This temperature rise occurs because the tungsten particle gives up its energy on impact to a small region in the stainless steel directly beneath the particle.

NASA

- I. Spitzig, William A.
- II. Grisaffe, Salvatore J.
- III. NASA TN D-2461

"The aeronautical and space activities of the United States shall be conducted so as to contribute . . . to the expansion of human knowledge of phenomena in the atmosphere and space. The Administration shall provide for the widest practicable and appropriate dissemination of information concerning its activities and the results thereof."

—NATIONAL AERONAUTICS AND SPACE ACT OF 1958

NASA SCIENTIFIC AND TECHNICAL PUBLICATIONS

TECHNICAL REPORTS: Scientific and technical information considered important, complete, and a lasting contribution to existing knowledge.

TECHNICAL NOTES: Information less broad in scope but nevertheless of importance as a contribution to existing knowledge.

TECHNICAL MEMORANDUMS: Information receiving limited distribution because of preliminary data, security classification, or other reasons.

CONTRACTOR REPORTS: Technical information generated in connection with a NASA contract or grant and released under NASA auspices.

TECHNICAL TRANSLATIONS: Information published in a foreign language considered to merit NASA distribution in English.

TECHNICAL REPRINTS: Information derived from NASA activities and initially published in the form of journal articles.

SPECIAL PUBLICATIONS: Information derived from or of value to NASA activities but not necessarily reporting the results of individual NASA-programmed scientific efforts. Publications include conference proceedings, monographs, data compilations, handbooks, sourcebooks, and special bibliographies.

Details on the availability of these publications may be obtained from:

SCIENTIFIC AND TECHNICAL INFORMATION DIVISION
NATIONAL AERONAUTICS AND SPACE ADMINISTRATION
Washington, D.C. 20546